

SRC-TR-87-74

**CHEMICAL PROCESS SYSTEMS
LABORATORY**

Polymerization of Olefins Through
Heterogeneous Catalysis. III. Polymer
Particle Modelling with an Analysis of
Intraparticle Heat and Mass Transfer
Effects

by

S. Floyd
K. Y. Choi
T. W. Taylor
W. H. Ray

CHEMICAL PROCESS SYSTEMS ENGINEERING LABORATORY

POLYMERIZATION OF OLEFINS THROUGH HETEROGENEOUS
CATALYSIS. III. POLYMER PARTICLE MODELLING WITH AN
ANALYSIS OF INTRAPARTICLE HEAT AND MASS
TRANSFER EFFECTS

S. Floyd
K.Y. Choi
T.W. Taylor
W.H. Ray

A CONSTITUENT LABORATORY OF
THE SYSTEMS RESEARCH CENTER

THE UNIVERSITY OF MARYLAND
COLLEGE PARK, MARYLAND 20742

Polymerization of Olefins through Heterogeneous Catalysis. III. Polymer Particle Modelling with an Analysis of Intraparticle Heat and Mass Transfer Effects

S. FLOYD, K. Y. CHOI, T. W. TAYLOR and W. H. RAY*, *Department of Chemical Engineering, University of Wisconsin, Madison, Wisconsin 53706*

Synopsis

Propylene and ethylene polymerization in liquid and gas media are described by a multigrain particle model. Intraparticle heat and mass transfer effects are investigated for a range of catalyst activities. For slurry polymerization, intraparticle mass transfer effects may be significant at both the macroparticle and microparticle level; however, for normal gas phase polymerization, microparticle mass transfer effects appear more likely to be important. Intraparticle temperature gradients would appear to be negligible under most normal operating conditions.

INTRODUCTION

The kinetics of polymerization of olefins over heterogeneous catalysts is not yet understood in detail. There is still great controversy concerning the surface phenomena and the nature of the active centers for reaction. In addition, from a reaction engineering standpoint, it is of significance that the effects of heat and mass transfer limitations during polymerization have not been clarified. Recent theoretical and experimental studies by our research group¹⁻⁷ have dealt with questions of kinetics and physical transport limitations in these polymerizations. These and other studies provide evidence that, in some circumstances, significant diffusion resistance to monomer transport will exist, and this can mask the intrinsic rate constants of the catalyst. In addition to mass transfer effects, there exists the possibility of inadequate removal of the heat of polymerization from the growing polymer particle. This may result in temperature gradients within the particle.

In modern polyolefin processes which utilize highly active Ziegler-Natta catalyst systems, it is often reported that particle sintering or agglomeration occurs in the polymerization reactor due to poor heat removal from the reacting catalyst/polymer particles. This suggests that there may also exist a significant temperature difference between the solid phase and bulk fluid phase during the reaction. This series of papers will be concerned with the quantitative analysis of both external film and intraparticle heat and mass transfer limitations through detailed mathematical modelling.

Several recent papers have reported modelling studies with nonisother-

* Author to whom correspondence should be addressed

mal polymer particles. McGreavy and Rawlings⁹ simulated both particle fluid and intraparticle temperature nonuniformities and concluded from their model that nonisothermal effects could be important during the first 30–60 min of reaction. Nagel et al.¹ analyzed the temperature history of low activity catalysts (such as Stauffer AA 1.1) in slurry polymerization and concluded that temperature gradients in the particle were negligible. On the other hand, Wisseroth^{9,10} and Brockmeier¹¹ studied particle/fluid temperature differences and concluded that significant temperature differences could exist between the particle and the surrounding fluid under some circumstances. Choi et al.^{4,6,7} carried out a detailed analysis of nonisothermal effects and summarized their results at the 1982 IUPAC meeting.⁴ Most recently, Laurence and Chiovetta¹² analyzed heat and mass transfer effects and concluded that temperature transients are an important factor during catalyst breakup. Both Choi et al.^{4,6,7} and Laurence and Chiovetta¹² showed that the temperature inside the particle could reach the melting point of the polymer under some circumstances for gas phase polymerization. It is the purpose of the present series of papers to extend the analysis reported in Refs. 1 and 4 so as to more clearly define the conditions under which intraparticle gradients are expected to arise and when particle–fluid mass transfer limitations and particle overheating are expected to occur. This paper will deal with intraparticle gradients, and the companion paper will treat boundary layer heat and mass transfer resistances.

POLYMER PARTICLE MODELS

Polymer particles in Ziegler–Natta polymerization have several resistances to heat and mass transfer. Assuming the macroscopic reactor is completely mixed and at uniform temperature, the first heat and mass transfer resistances present are in the particle boundary layer. Next, monomer must diffuse through the particle to the catalyst active sites to react. Heat generated from the polymerization is transferred by conduction to the catalyst particle surface and then by convection through the boundary layer to the fluid. The analysis of this system is complicated by the fact that as the reaction proceeds polymer is formed and the particle grows.

The catalyst particle model used for detailed simulations of these effects is the multigrain model shown schematically in Figure 1. This model was originally suggested by Yermakov et al.¹³ to estimate concentration profiles in the polymer particle and has been used in our work^{1,2,6} to predict the yield and the molecular weight distribution of the polymer product. This model was also adopted by Laurence and Chiovetta¹² for detailed simulations of behavior at short times. The model structure is based on numerous experimental observations that the original catalyst particle quickly breaks up into many small catalyst fragments ("primary crystallites") which are dispersed throughout the growing polymer. Thus, the large macroparticle is comprised of many small polymer particles (microparticles), which encapsulate these catalyst fragments. In this idealized picture, all microparticles at a given large particle radius are assumed to be the same size. As illustrated in Figures 1–3, for monomer to reach the active sites, there is

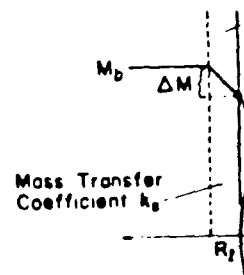
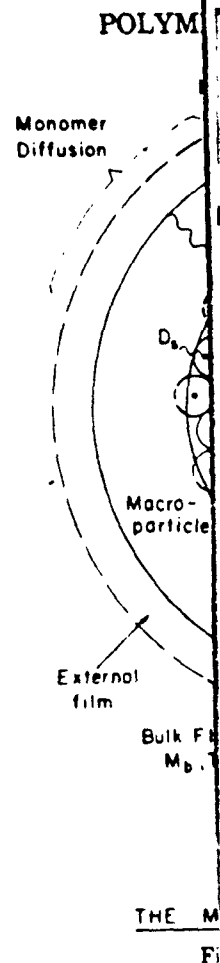


Fig. 2. Concentration profiles.

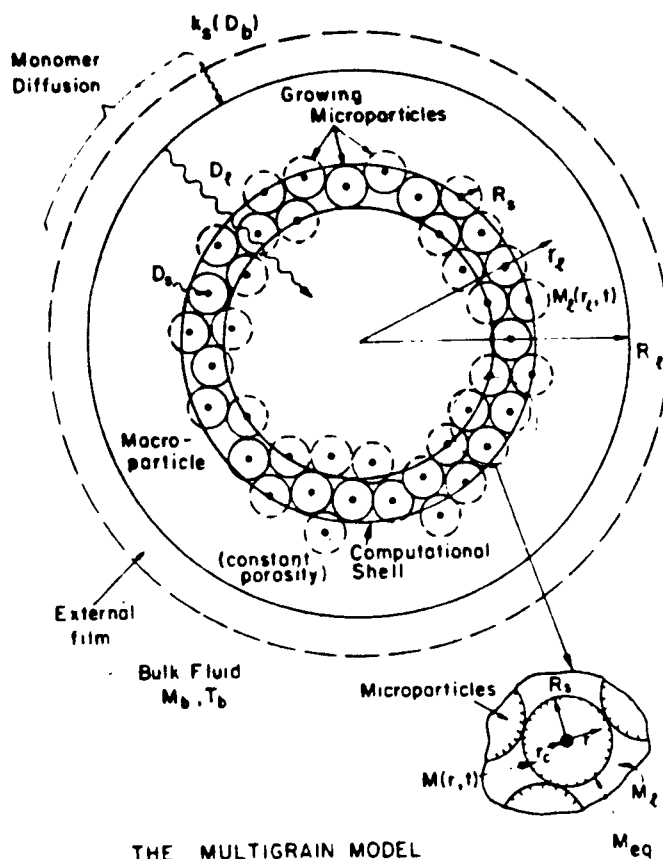


Fig. 1. The multigrain model.

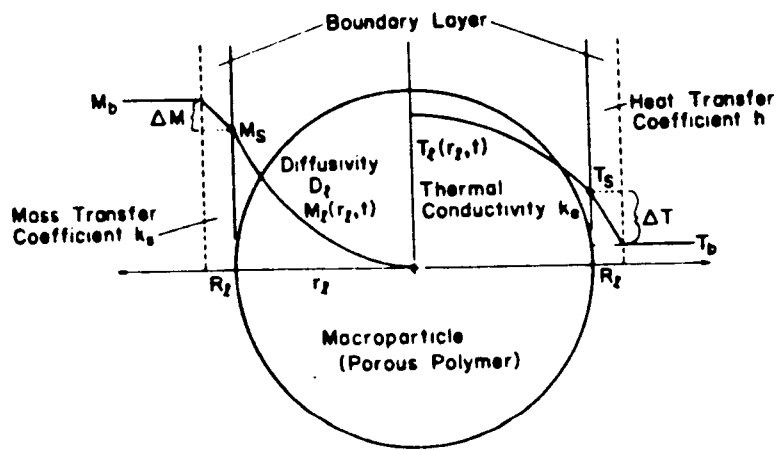


Fig. 2 Concentration and temperature gradients in the macroparticle.

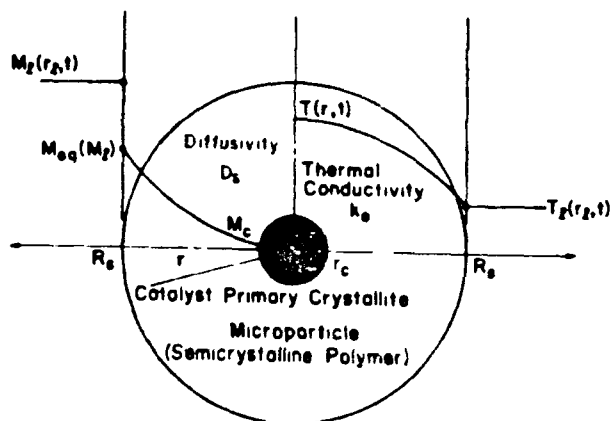


Fig. 3. Concentration and temperature gradients in the microparticle.

both macrodiffusion in the interstices between microparticles and microdiffusion within the microparticles. In general, the effective diffusion coefficients for the two regimes are not equal. We also include the possibility of an equilibrium sorption of monomer at the surface of the microparticle.

Material Balances

To model the particle, relations must be developed between the monomer concentrations in the large and small particles and the radial shell growth, particle yield, and temperature. The governing equation for the diffusion of monomer in the macroparticle is

$$\epsilon_l \frac{\partial M_l}{\partial t} = \frac{1}{r_l^2} \frac{\partial}{\partial r_l} \left(D_l r_l^2 \frac{\partial M_l}{\partial r_l} \right) - R_r \quad (1)$$

where ϵ_l is the large particle porosity, $M_l(r_l, t)$ is the monomer concentration in the pores of the macroparticle, and D_l is the pseudobinary macrodiffusion coefficient. The reaction rate term R_r represents the total rate of consumption of monomer in an infinitesimal spherical shell at a given radius of the macroparticle. The boundary and initial conditions are

$$r_l = 0, \quad \frac{\partial M_l}{\partial r_l} = 0 \quad (2)$$

$$r_l = R_l, \quad D_l \frac{\partial M_l}{\partial r_l} = k_s (M_b - M_l) \quad (3a)$$

or

$$r_l = R_l, \quad M_l = M_s \quad (3b)$$

$$t = 0, \quad M_l = M_{l0} \quad (4)$$

where M_b is the bulk monomer concentration at the external surface of the macroparticle. For the microparticle

where $M(r, t)$ is the monomer concentration in the microparticle, M_c is the monomer concentration at the catalyst core at $r = r_c$, by

where boundary conditions at the surface of the microparticle, $r = R_s$, are

where k_p is the propagation rate constant, M_c is the monomer concentration at the catalyst sites, and M_s is the monomer concentration at the surface of the microparticle.

As mentioned above, the microparticle is assumed to be impermeable to the monomer. The polymerization reaction takes the form

$$\rho_p C_p$$

with boundary conditions

$$r =$$

where M_b is the bulk monomer concentration in the reactor, k_s is the mass transfer coefficient in the external film, and M_s is the monomer concentration at the external solid surface.

For the microparticles, the monomer diffusion equation is given as

$$\epsilon_s \frac{\partial M}{\partial t} = \frac{1}{r^2} \frac{\partial}{\partial r} \left(D_s r^2 \frac{\partial M}{\partial r} \right) \quad (5)$$

$$r_c \leq r \leq R_s$$

where $M(r, t)$ is the monomer concentration in the microparticle, D_s is the pseudobinary microdiffusion coefficient, and ϵ_s is the porosity. In the microparticles, all of the active sites are assumed to be at the surface of the catalyst core at $r = r_c$. Thus, the boundary and initial conditions are given by

$$r = r_c, \quad 4\pi r_c^2 D_s \frac{\partial M}{\partial r} = \frac{4}{3} \pi r_c^3 R_p \quad (6)$$

$$r = R_s, \quad M = M_\infty(M_s) \leq M_b \quad (7)$$

$$t = 0, \quad M = M_{s0} \quad (8)$$

where boundary condition (7) allows for the possibility of a sorption equilibrium at the surface of the microparticles. Here r_c is the catalyst primary particle radius, R_s is the microparticle radius, and R_p is the rate of polymerization at the catalyst particle surface given by

$$R_p = k_p C_* M_c \quad (9)$$

where k_p is the propagation rate constant, C_* is the concentration of active catalyst sites, and M_c is the monomer concentration at the catalyst surface.

Energy Balances

As mentioned above, the microparticle consists of a solid catalyst core assumed to be impermeable and encapsulated by a catalyst-free polymer shell. The polymerization reaction occurs only at the external surface of the catalyst core. Analogous to eq. (5), the microparticle energy balance takes the form

$$\rho_p C_p \frac{\partial T}{\partial t} (r, t) = k_s \left[\frac{1}{r^2} \frac{\partial}{\partial r} \left(r^2 \frac{\partial T}{\partial r} \right) \right] \quad (10)$$

$$r_c < r \leq R_s$$

with boundary conditions

$$r = r_c, \quad -4\pi r_c^2 k_s \frac{dT}{dr} = (-\Delta H_p) \frac{4}{3} \pi r_c^3 R_p \quad (11)$$

$$r = R_s, \quad T = T_b \quad (12)$$

Similarly, an energy balance over the macroparticle takes the form

$$\rho_p C_p \frac{\partial T_i}{\partial t} = \left[\frac{1}{r_i^2} k_e \frac{\partial}{\partial r_i} \left(r_i^2 \frac{\partial T_i}{\partial r_i} \right) \right] + (-\Delta H_p) R_v \quad (13)$$

$$0 < r_i < R_i$$

where the volumetric reaction rate R_v may include the effects of micro-particle heat and mass transfer resistance. For the macroparticle, the boundary and initial conditions are

$$r_i = 0, \quad \frac{\partial T_i}{\partial r_i} = 0 \quad (14)$$

$$r_i = R_i, \quad k_e \frac{\partial T_i}{\partial r_i} = h [T_b - T_i] \quad (15a)$$

or

$$r_i = R_i, \quad T_i = T_s \quad (15b)$$

$$t = 0, \quad T_i = T_{i0} \quad (16)$$

These equations must be solved together with eqs. (1-4) to predict the concentration and temperature distribution in the macroparticle. This is illustrated pictorially in Figures 2 and 3.

Particle Parameter Values

In the analysis to follow, the practical conclusions will depend on the range of parameter values one might encounter for a polymer particle. For ethylene polymerization and propylene polymerization in slurry or gas phase reactors, these are tabulated in Table I. For some parameters (e.g., for k_p , C_s , D_s , D_i , R_s , R_i) there are a range of values which arise, and this range is indicated in the table. Both the microscale pseudobinary diffusivity D_s and macroscale pseudobinary diffusivity D_i play crucial roles in estimating intraparticle temperature and concentration gradients. However, it is difficult to determine the value of these diffusivities precisely. Thus let us discuss how one may arrive at the most likely values.

For macroscale diffusion through the interstices between the microparticles, we may estimate the effective diffusivity D_i as one would for more conventional heterogeneous catalysts.¹⁴ The effective diffusion coefficient in a solid may be represented by the bulk diffusivity in the fluid, D_b , multiplied by ϵ/τ , where ϵ is the porosity of the solid and τ is a "tortuosity factor", i.e., $D_i = D_b(\epsilon/\tau)$. In liquid slurry polymerization, the slurry diluent permeates the pores of the macroparticle and the appropriate bulk diffusivity, D_b , is the diffusivity of monomer in the diluent, which is of the order of 8×10^{-5} cm²/s under industrial conditions (see Table I). The porosity of the catalyst or polymer particle is 0.4 or less, and values of τ in the range 2-7 are common.¹⁴ Thus, the value of macroparticle diffusivity for slurry polymerization would be in the range of $10^{-6} \leq D_i \leq 10^{-5}$ cm²/s. For gas

TABLE I
Reaction Conditions, Thermal, Physical and Transport Properties for Polymerization of Propylene and Ethylene Under Industrial Conditions

Property	Propylene (PP)		Ethylene (PE)		References
	Slurry (n-heptane)	Gas	Slurry (n-hexane)	Gas	
Mol. wt. L ¹	40	1.0	2.0	1.0	6
T, K	343	343	353	353	6
P, atm	11	21	28	27	19
Mol. fraction monomer	0.49	1	0.26	1	19,22
		0.4	22.7	25.7	17,18,23

TABLE I
Reaction Conditions, Thermal, Physical and Transport Properties for Polymerization of Propylene and Ethylene Under Industrial Conditions

Property	Propylene (PP)		Ethylene (PE)		References
	Slurry (n-heptane)	Gas	Slurry (n-hexane)	Gas	
M_p (mol/L) ^a	4.0	1.0	2.0	1.0	6
T_p (K) ^a	343	343	353	353	6
P (atm) ^a	11	21	28	27	19
Mol fraction monomer	0.49	1	0.26	1	19,22
$-\Delta H_p$ (kcal/mol)	20.5	24.8	22.7	25.7	17,18,23
ρ (g/cm ³) ^a	0.3	0.3	0.3	0.3	17,18
E_p (kcal/mol)	10	10	10	10	6
k_p (L/mol site s)	660-2640	2640	2000-4000	4000	6
(high activity catalyst)					
C_p (mol sites/L cat)	10^3-10^4	10^3-10^4	10^3-10^4	10^3-10^4	6
k_d (cal cm s k)	2.5×10^4	5×10^5	2.3×10^4	7×10^5	18
k_p (cal/cm s K) ^b	3.5×10^4	2.6×10^4	5.6×10^4	4.8×10^4	17,18,20
ρ_p (g/cm ³)	0.905	0.905	0.96	0.96	17
ρ_s (g/cm ³)	0.64	—	0.61	—	18
ρ_l (g/cm ³)	0.46	0.042	0.38	0.028	18,21
ρ_g (g/cm ³)	0.58	—	0.576	—	18
μ_p (cp)	0.242	—	0.184	—	18
μ_s (cp)	0.07	0.01	0.07	0.012	20
μ_l (cp)	0.135	—	0.149	—	14,15
D_p (cm ² /s)	8×10^5	4×10^3	1×10^4	6×10^{-3}	16
D_s (cm ² /s)	10^6-10^5	10^4-10^3	10^6-10^5	10^4-10^3	16
D_l (cm ² /s)	10^6-10^5	10^6-10^6	10^6-10^6	10^6-10^6	16
R_p (cm ³ /s)	10^6-10^4	10^6-10^4	10^6-10^4	10^6-10^4	16
R_s (cm ³ /s)	10^4-10^1	10^4-10^1	10^4-10^1	10^4-10^1	16

^a Values correspond to conditions of industrial operation^{22,24} (pressures may be higher or lower for individual processes).

^b Calculated using Russell's equation²⁰ with a porosity of 0.37.

^c Calculated using the Kenda-Monroe equation.²¹

^d Polymerizing particles grow in diameter by a factor of 10 or more compared to original catalyst size. Some modern catalysts are capable of producing polymer particles 2 mm or more in diameter.²⁴

cm^2/s for vapors such as *n*-hexane, cyclohexane, and benzene. The value of D_0 in amorphous polypropylene was somewhat lower in the case of benzene. The diffusion coefficient for such vapors depends significantly on the concentration; Michaels and Bixler²⁷ found that the diffusion coefficient increased by 2 orders of magnitude between zero penetrant concentration and saturation for vapors such as benzene and hexane in polyethylenes at 25°C. For linear polyethylenes, the measured D_s values at saturation were of the order of $10^{-7} \text{ cm}^2/\text{s}$. D_s for heptane in polypropylene was found to be $\sim 10^{-8} \text{ cm}^2/\text{s}$ at reaction conditions.³³ In slurry polymerization, the microparticles are in contact with the diluent liquid and are probably saturated by it. Thus, swelling may be considered to occur, and the microdiffusion coefficient might be higher than for gas phase polymerization.

In summary, it is reasonable to surmise that the value of D_s lies in the range 10^{-8} – $10^{-6} \text{ cm}^2/\text{s}$ for diffusion of monomer ethylene or propylene in polyethylene or polypropylene and copolymers under reaction conditions. For highly isotactic polypropylene or high density polyethylene, the lower end of the range would apply, while for copolymers (such as ethylene-propylene copolymers) the upper end would apply. Polymerization at low temperatures would mean lower values of D_s , while polymerization at high temperatures would indicate higher D_s values. Because increased monomer sorption increases D_s , polymerizing under high pressures in gas phase or slurry would give higher D_s values while low pressure lab reactors should have a lower D_s value. Also since diluents such as heptane or hexane also swell the polymer and aid diffusion, slurry phase values of D_s would be expected to be larger than for gas phase polymerization. Obviously larger comonomers such as hexane and octene would have diffusivities towards the lower end of the range of D_s . Higher values of the diffusivity would be expected for hydrogen, ($D_s \sim 10^{-6}$) while smaller values are anticipated for diffusion of organoaluminum compounds. For HDPE or highly isotactic polypropylene at typical industrial temperatures and pressures in gas phase, one would expect D_s to lie in the range 1 – $5 \times 10^{-8} \text{ cm}^2/\text{s}$.

An additional issue is the process of sorption of monomer (or other fluids) by the polymer of the microparticles. According to Michaels and Bixler,³¹ there is negligible sorption in the crystalline portion of the polymer although macroscopically the polymer is completely homogeneous and isotropic with respect to dissolution and diffusion. Thus, the solubility in partially crystalline polymer will be proportional to the amorphous content. From the work by Michaels and Bixler,³¹ one may approximately model the equilibrium sorption of monomers from the *gas phase* as

$$M_{eq} = kP$$

where k is a Henry's law constant and P is the gas partial pressure in the pores. For partially crystalline polymer, $k = \alpha k^*$, where α is the amorphous content of the polymer and k^* is the solubility constant for purely amorphous polymer. From literature data,^{28,31} values of k^* are $\sim 0.04 \text{ mol/L atm}$ for solubility of ethylene in polyethylene and $\sim 0.16 \text{ mol/L atm}$ for propylene in polyethylene. Values of k^* for propylene in polypropylene are probably comparable. From the experiments in Ref. 31, the solubility of

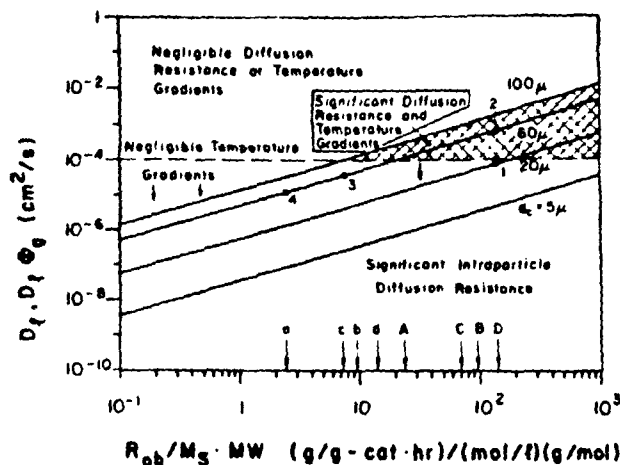


Fig. 9. Regimes for macroparticle diffusion resistance and temperature gradients. $D_i \Phi_g$ vs. observed catalyst activity. Approximate values for typical catalyst if $M_s = M_b$: (a,A) propylene slurry polymerization, low and high activity catalyst; (b,B) propylene gas phase polymerization, low and high activity catalyst; (c,C) ethylene slurry polymerization, low and high activity catalyst; (d,D) ethylene gas phase polymerization, low and high activity catalyst (low activity, $R_{ob} = 400$ g/g cal h, high activity, $R_{ob} = 4000$ g/g cal h under representative industrial conditions).

0.02, in terms of the polymerization parameters. Here we may define an overall observed reaction rate R_{ob} , which accounts for both microparticle and macroparticle diffusion limitations as well as for equilibrium sorption

$$R_{ob} = \eta_i \eta_s \eta_{eq} R_{kin} \quad (40)$$

where R_{kin} is defined by eq. (24) with $T_{ref} = T_s$, $M_{ref} = M_s$ in this case. Using the definition of α_i , we see that

$$\alpha_i = \left(\frac{\rho_c R_{ob} (R_c)^2}{3.6 M_s MW D_i \Phi_g \eta_i} \right)^{1/2} \quad (41)$$

so that lines corresponding to $\alpha_i = 1$, $\eta_i = 1$ can be represented in simple terms. Also plotted is the line $D_i = 10^{-4}$ corresponding to the criterion $\beta < 0.02$ for which there are negligible temperature gradients. Note that it is only for extremely high catalyst activities and large catalyst particles that significant macroparticle temperature gradients could exist (indicated by curves in the shaded region of Figure 9).

To illustrate how to use Figure 9, suppose that one has a 20 μ m diameter catalyst particle with $R_{ob} = 4000$ g/g cat h for ethylene gas phase polymerization when the ethylene pressure is 27 atm ($M_b \approx 1$ mol/L). If we assume $M_s = M_b$, then $R_{ob}/M_s MW = 143$. Thus this catalyst corresponds to point 1 in Figure 9 where $D_i \Phi_g = 10^{-4}$, $D_i = 10^{-4}$. Thus, for $D_i \Phi_g$ values $> 10^{-4}$, there is negligible heat and mass transfer resistance in the macroparticle. If we assume $D_i \sim 10^{-4}$ as a conservative estimate, then we conclude that there will be no significant internal concentration and

temperature gradients in diameter catalyst particle will be expected to have $D_i \Phi_g > 10^{-3}$. The significant internal temperature had grown by a factor

If we consider gas phase catalyst of the Stauffer type represented by point 3 $\sim 5 \times 10^{-5}$ for the onset of gas phase, we will have R_{ob} in the macroparticle for diameter catalyst for the observed productivity, $R_{ob} D_i = 10^{-5}$, $D_i \Phi_g = 10^{-6}$ $10^{-6} \leq D_i \leq 10^{-5}$ cm²/s in the macroparticle; heat will be significant mass the particle size exceeded.

Having shown that in the macroparticle unanalyze for macroparticle an isothermal particle. (37) has the solution

where z and α_i are defined factor, η_i , defined by eq.

From the definition of (41) and (42) graphically catalyst particles, one smaller catalyst particle catalyst particle size, growth factor Φ_g .

It is interesting to note in propylene slurry (e.g. size of 60 μ m), reasonable to cause macroparticle productivity catalyst in gas not expect to see macroparticle 10, where a catalyst particle polymerization with a high is true for high activity

temperature gradients in the macroparticle. However, note that a 60 μm diameter catalyst particle with the same observed productivity (point 2) will be expected to have negligible internal heat and mass transfer resistance for $D_l\Phi_p > 10^{-3}$. Thus if we assume $D_l = 10^{-4}$, then one would expect significant internal temperature and concentration gradients until the polymer had grown by a factor of 10 ($\Phi_p = 10$).

If we consider gas phase propylene polymerizations with a low activity catalyst of the Stauffer AA type with a catalyst diameter of 60 μm , this is represented by point 3 in Figure 9 corresponding to $D_l\Phi_p$, D_l values of $\sim 5 \times 10^{-5}$ for the onset of diffusion resistance. Thus since $D_l > 10^{-4}$ for gas phase, we will have negligible temperature and concentration gradients in the macroparticle for this catalyst in gas phase. If we use a 60 μm diameter catalyst for the slurry polymerization of propylene with the same observed productivity, R_{ob} , this corresponds to point 4 in Figure 9 where $D_l = 10^{-5}$, $D_l\Phi_p = 10^{-5}$ for the onset of diffusion resistance. For slurry $10^{-6} \leq D_l \leq 10^{-5}$ cm^2/s . Thus there will not be any temperature gradients in the macroparticle; however, with an actual value of $D_l \sim 10^{-6}$, there will be significant mass transfer resistance due to diffusion—at least until the particle size exceeds $\Phi_p > 10$.

Having shown that intraparticle temperature gradients will be negligible in the macroparticle under most normal operating conditions, we may now analyze for macroparticle mass transfer limitations in more detail assuming an isothermal particle. For this case, the macroparticle material balance (37) has the solution

$$c = \sinh(\alpha_l z)/z \sinh(\alpha_l)$$

where z and α_l are defined by Eq. (38). Thus, the macroparticle effectiveness factor, η_l , defined by eq. (39), has the solution⁴¹

$$\eta_l = \frac{3}{\alpha_l} \left[\frac{1}{\tanh(\alpha_l)} - \frac{1}{\alpha_l} \right] \quad (42)$$

From the definition of α_l , R_{ob} in eqs. (40) and (41) one may represent eqs. (41) and (42) graphically as shown in Figures 10–12. Note that, for larger catalyst particles, one expects more serious diffusion limitations than for smaller catalyst particles at the same growth factor. However, for a fixed catalyst particle size, diffusion limitations are reduced with increasing growth factor Φ_p .

It is interesting to note from Figure 11 that for a low activity catalyst in propylene slurry (e.g., Stauffer AA type catalyst with average catalyst size of 60 μm), reasonable values of D_l (e.g., 10^{-6} – 10^{-5} cm^2/s) are sufficient to cause macroparticle diffusion limitations. However, for the same productivity catalyst in gas phase (where $D_l \approx 10^{-4}$ – 10^{-3} cm^2/s), one would not expect to see macroparticle diffusion limitations. As indicated in Figure 10, where a catalyst particle size of $d_p = 20$ μm is used for ethylene polymerization with a high activity catalyst, one sees that the same conclusion is true for high activity catalysts; i.e., the possibility of significant intra-

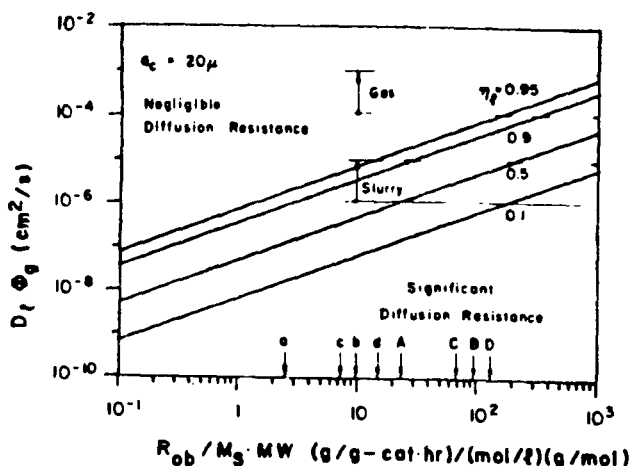


Fig. 10. Regimes for isothermal macroparticle diffusion resistance. $D_i \Phi_g$ vs. observed catalyst activity for catalyst with initial particle size $d_c = 20 \mu\text{m}$. Approximate values for typical catalyst if $M_S = M_A$: (a,A) propylene slurry polymerization, low and high activity catalyst; (b,B) propylene gas phase polymerization, low and high activity catalyst; (c,C) ethylene slurry polymerization, low and high activity catalyst; (d,D) ethylene gas phase polymerization, low and high activity catalyst (low activity, $R_{ob} = 400 \text{ g/g cat h}$, high activity, $R_{ob} = 4000 \text{ g/g cat h}$ under representative industrial conditions).

particle concentration gradients for slurry polymerization, but not for gas phase polymerization. However, as indicated in Figure 12, for gas phase polymerization with large high activity catalysts, internal concentration gradients can be significant. Furthermore, if catalyst activity continues to improve and catalyst particle sizes increase dramatically, then internal gradients will become even more significant in gas phase processes.

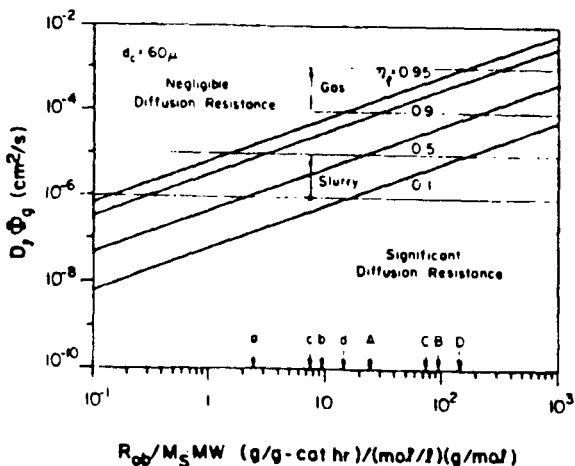


Fig. 11. Regimes for isothermal macroparticle diffusion resistance. $D_i \Phi_g$ vs. observed catalyst activity for catalyst with initial particle size $d_c = 60 \mu\text{m}$. Approximate values for typical catalysts if $M_S = M_A$: (a,A) propylene slurry polymerization, low and high activity catalyst; (b,B) propylene gas phase polymerization, low and high activity catalyst; (c,C) ethylene slurry polymerization, low and high activity catalyst; (d,D) ethylene gas phase polymerization, low and high activity catalyst (low activity, $R_{ob} = 400 \text{ g/g cat h}$, high activity, $R_{ob} = 4000 \text{ g/g cat h}$ under representative industrial conditions).

Fig. 12. Regimes for isothermal macroparticle diffusion resistance. $D_i \Phi_g$ vs. observed catalyst activity for catalyst with initial particle size $d_c = 20 \mu\text{m}$. Approximate values for typical catalyst if $M_S = M_A$: (a,A) propylene slurry polymerization, low and high activity catalyst; (b,B) propylene gas phase polymerization, low and high activity catalyst; (c,C) ethylene slurry polymerization, low and high activity catalyst; (d,D) ethylene gas phase polymerization, low and high activity catalyst (low activity, $R_{ob} = 400 \text{ g/g cat h}$, high activity, $R_{ob} = 4000 \text{ g/g cat h}$ under representative industrial conditions).

It is clear from Figure 12 that the diffusion resistance could manifest itself in gas phase polymerization, as has been observed for low activity. Note that catalyst particle size for slurry polymerization is small and overall yield for high activity catalyst is high.

In this paper quantitative estimates of M_S are given in graphical form to allow comparison of temperature and concentration gradients. Because of the large particle sizes, these criteria are significant when there is a significant macroparticle diffusion resistance. Similarly, quantitative estimates of M_S are given in graphical form to allow comparison of temperature and concentration gradients. Because of the large particle sizes, these criteria are significant when there is a significant macroparticle diffusion resistance. Similarly, quantitative estimates of M_S are given in graphical form to allow comparison of temperature and concentration gradients. Because of the large particle sizes, these criteria are significant when there is a significant macroparticle diffusion resistance.

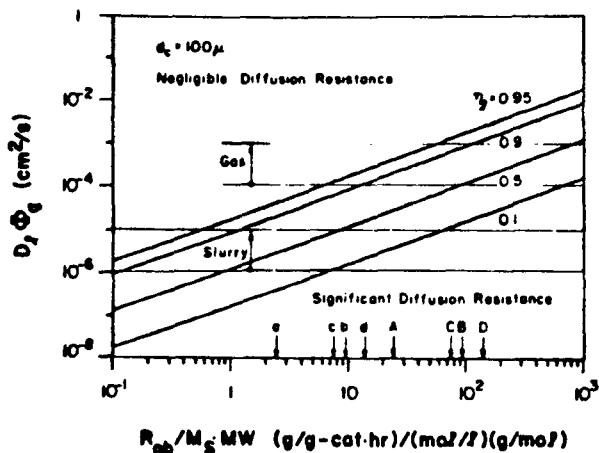


Fig. 12. Regimes for isothermal macroparticle diffusion resistance. $D_p \Phi_p$ vs. observed catalyst activity for catalyst with initial particle size $d_p = 100 \mu\text{m}$. Approximate values for typical catalyst if $M_s = M_p$: (a,A) propylene slurry polymerization, low and high activity catalyst; (b,B) propylene gas phase polymerization, low and high activity catalyst; (c,C) ethylene slurry polymerization, low and high activity catalyst; (d,D) ethylene gas phase polymerization, low and high activity catalyst (low activity, $R_{ob} = 400 \text{ g/g cat h}$, high activity, $R_{ob} = 4000 \text{ g/g cat h}$ under representative industrial conditions).

It is clear from Figures 10–12 that as the polymer particle size increases, the diffusion resistance becomes smaller. Thus, diffusion control in slurry could manifest itself in terms of an acceleration or hybrid-type rate behavior, as has been observed under many circumstances, even for catalysts of low activity. Note that these results predict that a significant effect of catalyst particle size on the polymerization rate may be anticipated for slurry polymerization. This effect would primarily be seen in the initial rate for low activity catalyst, but there could be a significant effect on the overall yield for high activity catalysts.

CONCLUSIONS

In this paper quantitative criteria have been developed and presented in graphical form to allow one to evaluate the extent of intraparticle concentration and temperature gradients in polymer particles during olefin polymerization. Because we use observed reaction rates as a measure of catalyst activity, these criteria may underestimate microparticle diffusion limitations when there is significant resistance due to sorption equilibrium or macroparticle diffusion unless one uses good estimates of M_{eq} in Figures 5 and 6. Similarly, macroparticle diffusion resistance may be underestimated if there is a significant boundary layer mass transfer resistance unless good estimates of M_s are used in Figures 9–12.

From the analysis presented, it may be concluded that under most conditions normally encountered in industry or the laboratory, *intraparticle temperature gradients* should be negligible for both the microparticles and the macroparticles in gas or slurry polymerization reactors. Exceptions would be for large highly active catalyst particles early in the lifetime of the polymer particles in gas phase reactors. On the other hand, *intraparticle concentration gradients* in the microparticles can be significant for high

activity catalyst systems having large primary crystallites of catalyst, especially in gas phase polymerization. By contrast, *concentration gradients* in the *macroparticles* will normally be negligible for gas phase polymerization, but are expected to be significant in many slurry systems, even for catalysts of relatively low activity. For gas phase reactors, concentration gradients in the macroparticle could be important for high activity catalysts of large size especially early in the life time of the polymer particle. As the polymer particle grows, this macroparticle diffusion resistance will be reduced, contrary to some suggestions in the literature which ascribe the catalyst rate decay to an increase in the resistance to monomer transfer. Diffusion control in these systems can be detected by an acceleration type rate behavior, or by an effect of catalyst particle size on the rate or yield.

The sequel will discuss the question of heat and mass transport resistances in the particle boundary layer. More general conclusions regarding the importance of heat and mass transfer resistances will also be presented in a companion paper.

The analysis of heat and mass transfer resistance in the microparticle has assumed a spherical microparticle (globular microstructure). For cases of other microparticle morphologies, this will serve as an approximation. Further detailed modelling of other structures would be worthwhile if the present analysis suggests that microscale diffusion limitations may be important.

The authors are grateful to the National Science Foundation and to the following companies for research support: Exxon, DuPont, Mobil and Novacor, Ltd.

APPENDIX: NOMENCLATURE

A_p	surface area of polymer particle
c	dimensionless monomer concentration = M_1/M_s
C_p	heat capacity of polymer
C_{pf}	heat capacity of fluid
C_a	concentration of active sites (mol sites/L cat)
d_c	diameter of catalyst particle
d_p	diameter of polymer particle
D_0	diffusivity at zero penetrant concentration
D_b	bulk diffusivity of monomer
D_i	effective diffusivity in macroparticle
D_m	effective diffusivity in microparticle
E	activation energy for propagation (cal/mol)
ΔH_p	heat of polymerization (cal/mol)
h	external film heat transfer coefficient (cal/cm ² s K)
k	solubility constant (mol/L atm)
k^*	solubility constant for purely amorphous polymer (mol/L atm)
k_p	thermal conductivity of polymer particle (cal/cm s K)
k_f	thermal conductivity of fluid (cal/cm s K)
k_p	propagation rate constant (L/mol sites s)
k_e	external film mass transfer coefficient (cm/s)
M	monomer concentration in microparticle
M_b	bulk monomer concentration
M_c	monomer concentration at catalyst surface
M_m	monomer concentration at surface of microparticle
M_p	monomer concentration in pores of macroparticle
M_s	monomer concentration at macroparticle surface
ΔM	concentration drop across external film (mol/L)

MW	molecular weight of monomer
Nu	Nusselt number = hd_p/k_f
p	pressure (atm)
r	microparticle radius
r_1	macroparticle radius
r_c	catalyst primary crystallite radius
R	gas constant = 1.987 cal/mol °K
R_c	radius of catalyst particle
R_p	rate of polymerization
R_{kin}	kinetic reaction rate
R_i	radius of macroparticle
R_{ob}	observed polymerization rate
R_m	radius of microparticle
R_v	volumetric reaction rate
Re	Reynolds number = $\rho u d_p/\mu$
Sc	Schmidt number = μ/D
Sh	Sherwood number = $h d_p/k_f$
T	temperature in microparticle
T_b	temperature in bulk fluid
T_c	temperature at catalyst surface
T_i	temperature in macroparticle
T_s	temperature at macroparticle surface
ΔT	temperature rise across particle-fluid interface
u	particle-fluid relative velocity
u_t	terminal velocity of particle
V_c	volume of catalyst particle
z	dimensionless radius

α_1	dimensionless modulus of elasticity
α_2	dimensionless modulus of elasticity
β_p	dimensionless modulus of elasticity
ϵ	porosity
γ	dimensionless activation energy
ϕ_p	microparticle growth factor
Φ	macroparticle growth factor
ρ	density of slurry liquid
ρ_c	density of catalyst particle
ρ_d	density of slurry droplet
ρ_m	density of monomer
ρ_p	density of polymer
μ_d	viscosity of slurry droplet
μ_m	viscosity of monomer
μ_s	viscosity of slurry liquid
η_{eq}	adsorption equilibrium constant
η_p	microparticle effectiveness factor
η_i	macroparticle effectiveness factor
θ	dimensionless temperature
τ	tortuosity factor
τ_M	time constant for monomer transfer
τ_T	time constant for temperature transfer

1 E. D. Nagel, V. A. (1980)

2 T. W. Taylor, K. Y.

MW	molecular weight of monomer
Nu	Nusselt number = hd_p/k_f
p	pressure (atm)
r	microparticle radius
r_i	macroparticle radius
r_c	catalyst primary crystallite radius
R	gas constant = 1.987 cal/mol K
R_c	radius of catalyst particle
R_m	rate of polymerization of catalyst surface
R_{km}	kinetic reaction rate
R_i	radius of macroparticle
R_{ob}	observed polymerization rate (g/g cat h)
R_s	radius of microparticle
R_v	volumetric reaction rate in macroparticle
Re	Reynolds number = $\rho u d_p/D_s$
Sc	Schmidt number = $\mu/\rho D_s$
Sh	Sherwood number = $k_f d_p/D_s$
T	temperature in microparticle
T_b	temperature in bulk fluid
T_c	temperature at catalyst surface
T_i	temperature in macroparticle
T_s	temperature at macroparticle surface
ΔT	temperature rise across external film
u	particle-fluid relative velocity
u_t	terminal velocity of particle
V_c	volume of catalyst particle
z	dimensionless radius = r_i/R_i

GREEK SYMBOLS

α_i	dimensionless modulus = $R_i \sqrt{\eta_i k_p (T_c) C_o / D_i \Phi_s^3}$
α_c	dimensionless modulus = $r_c \sqrt{k_p C_o / D_s}$
β_c	dimensionless modulus = $\sqrt{(-\Delta H_p) D_s / k_c}$
ϵ	porosity
γ	dimensionless activity energy = E/RT_s
ϕ_s	microparticle growth factor = R_s/r_c
Φ	macroparticle growth factor = R_i/R_c
ρ	density of slurry liquid
ρ_c	density of catalyst particle
ρ_d	density of slurry diluent
ρ_m	density of monomer
ρ_p	density of polymer
μ_d	viscosity of slurry diluent
μ_m	viscosity of monomer
μ	viscosity of slurry liquid
η_m	sorption equilibrium effectiveness factor
η_s	microparticle effectiveness factor
η_i	macroparticle effectiveness factor
θ	dimensionless temperature rise = $\gamma (T_i - T_s)/T_s$
τ	tortuosity factor
τ_M	time constant for concentration equilibrium
τ_T	time constant for temperature equilibrium

References

- 1 E. D. Nagel, V. A. Kirillov, and W. H. Ray, *Ind. Eng. Chem., Prod. Res. Dev.*, **19**, 372 (1980)
- 2 T. W. Taylor, K. Y. Choi, H. G. Yuan, and W. H. Ray, *Physical Chemical Kinetics of Liquid*

Phase Propylene Polymerization, Proceedings of the 1981 MMI Symposium on Transitional Metal Catalyzed Polymerizations, Midland, Plenum, New York, 1983.

3. H. G. Yuan, T. W. Taylor, K. Y. Choi, and W. H. Ray, *J. Appl. Polym. Sci.*, **27**, 1691 (1982).
4. K. Y. Choi, T. W. Taylor and W. H. Ray, *Proceedings 1982 IUPAC*, Amherst, MA, July 1982.
5. K. Y. Choi, T. W. Taylor and W. H. Ray, in *Proceedings Berlin Workshop on Polymer Reaction Engineering*, October, 1982, K. H. Reichert and W. Geisler, Eds., Hanser Verlag, Munich, 1982, p. 313.
6. T. W. Taylor, PhD thesis, University of Wisconsin, 1983.
7. K. Y. Choi, PhD thesis, University of Wisconsin, 1984.
8. C. McGreavy and N. Rawling, *4th International Symposium on Chemical Reaction Engineering, I*, IV-152, Dechema Heidelberg, 1976.
9. Karl Wisseroth, *Chem. Zg.*, **101**, 271 (1977).
10. Karl Wisseroth, private communication, 1982.
11. N. F. Brockmeier, private communication, 1982.
12. R. L. Laurence and M. G. Chiovetta, in Ref. 5, p. 73.
13. Yu. I. Yermakov, V. G. Mikhailchenko, V. S. Beskov, Yu. P. Grabovskii, and I. V. Emirova, *Plast. Massy*, **9**, 7 (1970).
14. C. N. Satterfield, *Mass Transfer in Heterogeneous Catalysis*, MIT Press, Cambridge, 1970.
15. R. C. Reid, J. M. Prausnitz, and T. K. Sherwood, *Properties of Gases and Liquids*, McGraw-Hill, New York, 1977.
16. S. Floyd, PhD thesis, University of Wisconsin, 1986.
17. H. V. Boenig, *Polyolefins: Structure and Properties*, Elsevier, Amsterdam, 1966.
18. R. W. Gallant, *Physical Properties of Hydrocarbons*, Gulf, Houston, 1968, Vol. 1.
19. G. E. Mann, M. S. thesis, University of Wisconsin, 1985.
20. R. H. Perry and C. H. Chilton, Eds., *Chemical Engineer's Handbook*, 5th ed., McGraw-Hill, New York, 1973.
21. E. W. Lyckman, C. A. Eckert and J. M. Prausnitz, *Chem. Eng. Sci.*, **20**, 685 (1965).
22. L. I. Chriswell, *Chem. Eng. Prog.*, (Apr.), p. 84, (1983).
23. F. Rodriguez, *Principles of Polymer Systems*, 2nd ed., McGraw-Hill, New York, 1982.
24. N. F. Brockmeier, "Latest Commercial Technology for Propylene Polymerization," paper presented at Michigan Molecular Institute, August 17-21, 1981.
25. C. Cipnani and C. A. Trischman, *Chem. Eng.*, **66** (May 17, 1982).
26. D. W. McCall and W. P. Slichter, *J. Am. Chem. Soc.*, **80**, 1861 (1958).
27. A. S. Michaels and H. J. Bixler, *J. Polym. Sci.*, **50**, 413 (1961).
28. N. N. Li and R. B. Long, *AIChE J.*, **15**(1), 73 (1969).
29. H. K. Frensdorff, *J. Polym. Sci.*, **A-2**, **1**, 341 (1964).
30. C. E. Rogers, V. Stannett, and M. Szwarc, *J. Polym. Sci.*, **45**, 61 (1960).
31. A. S. Michaels and H. J. Bixler, *J. Polym. Sci.*, **50**, 393 (1961).
32. F. W. Bovey, *Macromolecules—An Introduction to Polymer Science*, Academic, New York, 1979, Chap. 5.
33. R. B. Long, *Ind. Eng. Chem.*, **4**(4), 445 (1965).
34. C. W. Hock, *J. Polym. Sci.*, **A-1**, **4**, 3055 (1966).
35. J. Wristers, *J. Polym. Sci.*, *Polym. Phys. Ed.*, **11**, 1619 (1973).
36. L. A. M. Rodriguez and H. M. Van Looy, *J. Polym. Sci.*, **A-1**, **4**, 1971 (1966).
37. J. Wristers, *J. Polym. Sci.*, *Polym. Phys. Ed.*, **11**, 1601 (1973).
38. Z. W. Wilchinsky, R. W. Looney, and E. G. M. Tornqvist, *J. Catal.*, **28**, 351 (1973).
39. R. P. Nielsen, in *Transition Metal Catalyzed Polymerizations*, R. P. Quirk, Ed., Harwood Academic, New York, 1983, p. 47.
40. B. L. Goodall, in Ref. 39, p. 355.
41. R. Aris, *The Mathematical Theory of Diffusion and Reaction in Permeable Catalysts*, Oxford University Press, Oxford, 1975, Vol. I, p. 285-300.
42. P. B. Weisz and J. S. Hicks, *Chem. Eng. Sci.*, **17**, 265 (1962).

Received June 24, 1985

Accepted September 22, 1985

Synthesis of Aron

ALMERIA NATA
Weizman

Novel aromatic polyphosphates (methyl, phenyl) phosphonic and phase transfer catalysis. Mixtures of the polyphosphates when the chloromethyl group confers flame resistance to

Polycondensation of aromatic polyphosphates is important for achieving melt,¹ interfacial,² and solid state applications. Of the phosphonates (PPD) is the most widely used for its stability by bringing chloromethylphosphonate anism of melt polycondensation. These polyphosphonates that are generally used for performance plastics. In the present study bisphenols: 4,4'-sulfonylphenyl)propane (tetrahydroxy) with PPD and methylphosphonate characterized.

The influence of the molecular weight of the polymers obtained from the glass transition temperature of polyphosphonates and their compatibility and flame

* Present address: Merck & Co., Inc., P.O. Box 2000, Kenilworth, NJ 07033.

Journal of Applied Polymer Science, Vol. 20, 2960-2966 (1976)
© 1986 John Wiley & Sons, Inc.

up to $\sim 100 \mu\text{m}$; however, it may not be valid for slurry polymerization concentration transients in ultralarge particles. In this case, neglecting these transients provides a conservative bound on intraparticle temperature gradients; thus we shall use the QSSA in the analysis here.

By invoking the QSSA, one may combine eqs. (1)–(4) and (13)–(16) in their steady state form to yield the relationship for the intraparticle temperature rise in the macroparticle,

$$T_i(0) - T_s = \frac{(-\Delta H_p) D_i (M_s - M_i(0))}{k_c} \quad (30)$$

where T_s and M_s are the temperature and monomer concentrations at the surface of the macroparticle and $T_i(0)$ and $M_i(0)$ are the values at the center.

For the slurry polymerization of propylene and ethylene (using the range of parameters in Table I), one may obtain conservative estimates by assuming $M_i(0) = 0$ and $M_s = M_b$, to estimate the maximum temperature rise in the macroparticle. This analysis predicts at most a 2–3 K temperature rise for propylene polymerization, and less than 1 K for ethylene polymerization. The actual values will normally be considerably less than this, since the center particle monomer concentration value will not be zero and there may be mass transfer resistance in the external boundary layer which causes $M_s < M_b$. Detailed calculations indicate that for typical conditions in slurry even with high activity catalyst, the internal temperature rise is a fraction of a degree centigrade. Thus our analysis supports the assumption that macroparticle internal temperature gradients should be negligible for slurry polymerization.

The situation for gas-phase polymerization is much more complicated. First, for homopolymerization without the presence of an inert or chain transfer agent, mass transfer in the macropores would not be properly described by a diffusion process but would have a substantial convective transport contribution driven by a pressure gradient in the particle. However, this is an unusual case because most gas-phase reactors have inerts, chain transfer agents, and sometimes comonomer which allow macroscale counterdiffusion mass transfer to apply. To analyze this situation, we shall consider both cases.

First, we assume that convective mass transport in a one-component gas leads to a negligible intraparticle mass transfer resistance because the macropores are large ($\sim 1 \mu\text{m}$) and the absolute pressure is large (15–30 atm) so that the intraparticle pressure drop required to overcome convective flow resistance is a small fraction of the total pressure. Thus as a conservative bound we assume that $M_i = M_s$ everywhere in the macropores. In this case the macroscale reaction rate R_r is only a function of T_i and

$$R_r = \eta_i \eta_{eq} k_p (T_i) C_s M_s (R_r)^3 / (R_i)^3 \quad (31)$$

where η_i accounts for microparticle diffusion limitations, η_{eq} represents

the sorption equilibrium, η_{eq} . This means that eq.

where

$$z = \frac{r}{R_i}$$

$$\delta = \left(\frac{R_i}{R_{ob}} \right)^2$$

and the well-known exponential integral

$$\exp \left[-\frac{E}{RT} \right]$$

has been made. Equation (31) whose solution has been given by Danckwerts⁷ for center temperature, $\theta(0)$

then for the parameter Φ_r for a macroparticle will be $\Phi_r = R_i / R_r$ and $\delta = 1$, to obtain R_{ob} as

$$d_r = \frac{R_i}{R_r}$$

Here $\Phi_r = R_i / R_r$ is the Thiele modulus for the reaction rate derived from eq. (31). Note that for low to moderate internal temperature

the sorption equilibrium, and R_c is the radius of the original catalyst particle. This means that eq. (13) may be rewritten

$$\frac{1}{z^2} \frac{\partial}{\partial z} \left(z^2 \frac{\partial \theta}{\partial z} \right) + \delta e^\theta = 0 \quad (32)$$

$$\theta'(0) = 0$$

$$\theta(1) = 0$$

where

$$z = \frac{r_l}{R_l}, \quad \theta = \frac{E}{RT_s} \left(\frac{T_l - T_s}{T_s} \right), \quad (33)$$

$$\delta = \frac{(-\Delta H_p) \eta_s \eta_{eq} k_p (T_s) C_* M_s (R_l)^2 E}{1000 k_c R (T_s)^2 (R_l^3 / R_c^3)}$$

and the well-known exponential approximation

$$\exp \left[-\frac{E}{RT_s} \left(\frac{T_s - T_l}{T_l} \right) \right] \approx \exp \left[-\frac{E}{RT_s} \left(\frac{t_s - T_l}{T_s} \right) \right] \quad (34)$$

has been made. Equation (32) is the classical Frank-Kamenetski equation whose solution has been tabulated in Ref. 41. In particular, the particle center temperature, $\theta(0)$, is less than 0.1 for $\delta < 1$. Since

$$T_l(0) - T_s = \frac{\theta(0) T_s}{(E/RT_s)} \quad (35)$$

then for the parameters in Table I, the internal temperature rise in the macroparticle will be less than 2 K if $\delta < 1$ in the case where there is no macroparticle mass transfer limitation. Thus we may use the definition for δ and set $\delta = 1$, to obtain the relationship between catalyst diameter, and R_{ob} as

$$d_c = 2R_c = \left[\frac{14,400 k_c (T_s)^2 MW \Phi_g}{(-\Delta H_p)(E/R) \rho_c R_{ob}} \right]^{1/2} \quad (36)$$

Here $\Phi_g = R_l/R_c$ is the macroparticle growth factor and R_{ob} is an observed reaction rate derived from eq. (31). This is illustrated graphically in Figure 7. Note that for low to medium catalyst activities, there is no significant internal temperature rise if the catalyst particle is below 100 μm in di-

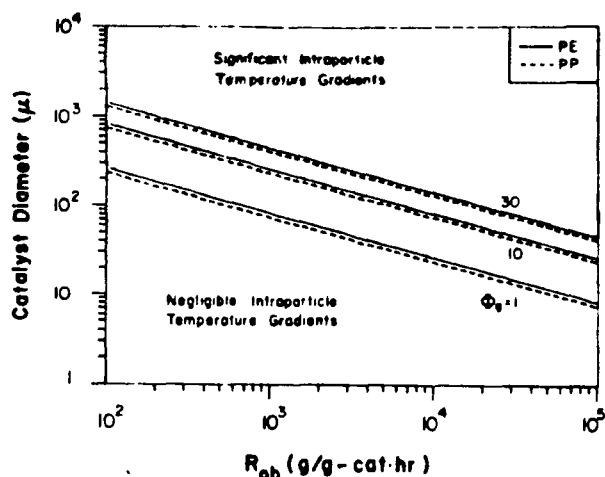


Fig 7. Regimes for significant macroparticle temperature gradients for ethylene and propylene polymerization. Catalyst size d_c vs. observed rate for various macroparticle growth factors $\Phi_g = R_i/R_s$.

ameter. However, for high catalyst activities (> 1000 g/g cat h), the catalyst particle diameter must be smaller to insure no internal temperature rise. This is a happy situation because, as catalyst activities increase, less catalyst is required for the same size polymer particle, and one naturally reduces the catalyst particle size. For the most active catalysts in use today, catalyst particle diameters below $20 \mu\text{m}$ would insure no intraparticle temperature gradients. Note that, as the polymer particle grows in size (i.e., Φ_g increases), intraparticle temperature gradients become less significant. In any case, the assumption of no mass transfer resistance is a very conservative bound. Thus one may conclude that, for one-component gas phase polymerization, there would be negligible internal temperature gradients in the macroparticle except for very large, high-activity catalyst particles.

Now let us consider the case where the presence of inerts, transfer agent, or slowly reacting comonomer requires a diffusion description of mass transfer in the macroparticle. Carrying out the bounding analysis using eq. (30) for gas phase polymerization is not as conclusive as it was for slurry. For the parameters in Table I, gas phase diffusivities can be higher than for slurry, so that, using eq. (30), large macroparticle temperature gradients cannot be ruled out. Thus more detailed studies of the gas phase situation are required.

If we put the macroparticle equations (1)–(4) and (13)–(16) in dimensionless form we obtain for the material balance

$$\frac{1}{z^2} \frac{\partial}{\partial z} \left(z^2 \frac{\partial c}{\partial z} \right) - \alpha \gamma c \exp \left(\frac{\theta}{1 + \theta/\gamma} \right) = 0, \quad 0 < z < 1 \quad (37)$$

$$\frac{dc(0)}{dz} = 0$$

$$c(1) = 1$$

where eqs. (1) and (25) ca

Here we have defined th

$$z = \frac{r}{R}$$

$$\gamma = \frac{1}{\beta}$$

$$c = \frac{1}{\alpha}$$

This is the classical nonisothermal situation. The solution to this equation may be applied to the macroparticle

$$\eta_1 = \frac{\text{reaction rate in pellet}}{\text{reaction rate in slab}}$$

For the parameters in Table I, factor plots for this range for $\alpha_1 < 1$, there is no significant temperature gradient in the pellet for the range $\beta = 0, \beta = 0.02$ are very significant temperature gradients in Table I for gas phase $10^{-4} \text{ cm}^2/\text{sec}$. Figure 9

10

 η_2 10

0.0

Fig 8. Nonisothermal factor plots corresponding to gas phase

where eqs. (1) and (25) can be combined to yield

$$\theta = \beta\gamma(1 - c)$$

Here we have defined the parameters

$$\begin{aligned} z &= \frac{r_1}{R_1}, \quad \alpha_1 = R_1 \left[\eta_1 \eta_\infty \frac{k_p(T_s) C_s}{D_1 \Phi_s^2} \right]^{1/2}, \\ \gamma &= \frac{E}{RT_s}, \quad \beta = \left(\frac{(-\Delta H_p) D_1 M_s}{k_s T_s} \right) \\ c &= \frac{M_1}{M_s}, \quad \theta = \left(\frac{T_1 - T_s}{T_s} \right) \gamma, \quad \Phi_s = \frac{R_1}{R_c} \end{aligned} \quad (38)$$

This is the classical nonisothermal reaction-diffusion problem whose solution has been tabulated many places (e.g., Refs. 41 and 42). The solution to this equation may be represented by an effectiveness factor η_1 which applies to the macroparticle and is defined by

$$\eta_1 = \frac{\text{reaction rate with macroscale diffusion}}{\text{reaction rate in absence of macroscale diffusion}} = \frac{3(dc/dz)_{z=1}}{(\alpha_1)^2} \quad (39)$$

For the parameters in Table I, $\gamma < 20$, and at most $\beta \approx 0.2$. The effectiveness factor plots for this range of parameters are shown in Figure 8. Note that, for $\alpha_1 < 1$, there is no significant diffusion limitation or temperature rise in the pellet for the range of β , $0 < \beta < 0.2$. Because the curves for $\beta = 0$, $\beta = 0.02$ are virtually superimposed, for $\beta < 0.02$, there is no significant temperature rise for any value of α_1 . For the parameter ranges in Table I for gas phase polymerization, one sees that $\beta < 0.02$ for $D_1 < 10^{-4}$ cm²/sec. Figure 9 provides a quick check on the criteria $\alpha_1 < 1$, $\beta <$

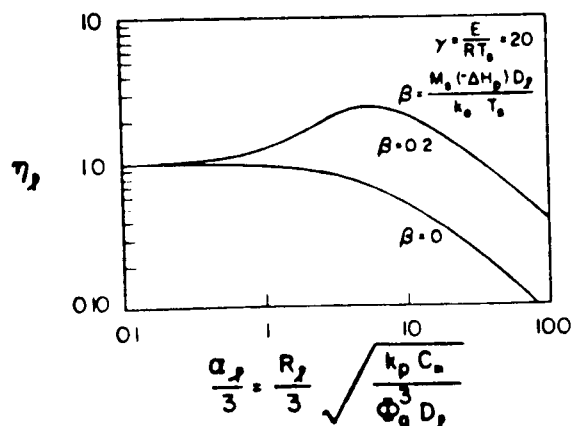


Fig 8 Nonisothermal macroparticle effectiveness factors for range of β , $0 < \beta \leq 0.2$, corresponding to gas phase olefin polymerization

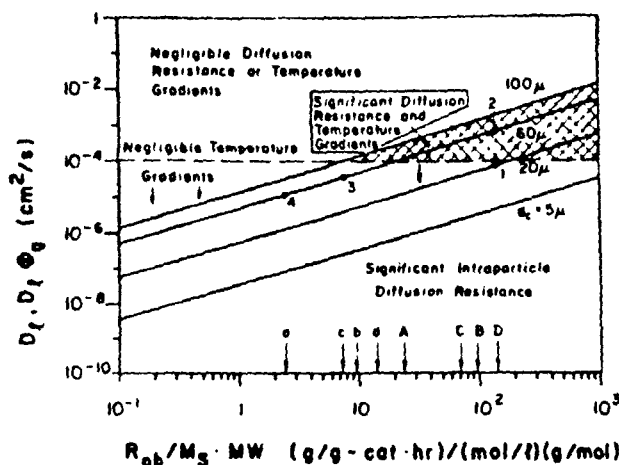


Fig. 9. Regimes for macroparticle diffusion resistance and temperature gradients. $D_i \Phi_g$ vs. observed catalyst activity. Approximate values for typical catalyst if $M_s = M_p$: (a,A) propylene slurry polymerization, low and high activity catalyst; (b,B) propylene gas phase polymerization, low and high activity catalyst; (c,C) ethylene slurry polymerization, low and high activity catalyst; (d,D) ethylene gas phase polymerization, low and high activity catalyst (low activity, $R_{ob} = 400$ g/g cal h, high activity, $R_{ob} = 4000$ g/g cal h under representative industrial conditions).

0.02, in terms of the polymerization parameters. Here we may define an overall observed reaction rate R_{ob} , which accounts for both microparticle and macroparticle diffusion limitations as well as for equilibrium sorption

$$R_{ob} = \eta_i \eta_r \eta_{eq} R_{kin} \quad (40)$$

where R_{kin} is defined by eq. (24) with $T_{ref} = T_s$, $M_{ref} = M_s$ in this case. Using the definition of α_i , we see that

$$\alpha_i = \left(\frac{\rho_r R_{ob} (R_r)^2}{3.6 M_s MW D_i \Phi_g \eta_i} \right)^{1.2} \quad (41)$$

so that lines corresponding to $\alpha_i \approx 1$, $\eta_i \approx 1$ can be represented in simple terms. Also plotted is the line $D_i = 10^{-4}$ corresponding to the criterion $\beta < 0.02$ for which there are negligible temperature gradients. Note that it is only for extremely high catalyst activities and large catalyst particles that significant macroparticle temperature gradients could exist (indicated by curves in the shaded region of Figure 9).

To illustrate how to use Figure 9, suppose that one has a 20 μ m diameter catalyst particle with $R_{ob} = 4000$ g/g cat h for ethylene gas phase polymerization when the ethylene pressure is 27 atm ($M_p \approx 1$ mol/L). If we assume $M_s = M_p$, then $R_{ob}/M_s MW = 143$. Thus this catalyst corresponds to point 1 in Figure 9 where $D_i \Phi_g = 10^{-4}$, $D_i = 10^{-4}$. Thus, for $D_i \Phi_g$ values $> 10^{-4}$, there is negligible heat and mass transfer resistance in the macroparticle. If we assume $D_i \sim 10^{-4}$ as a conservative estimate, then we conclude that there will be no significant internal concentration and

temperature gradients in diameter catalyst particle will be expected to have $D_i \Phi_g > 10^{-3}$. If significant internal temperature had grown by a factor

If we consider gas phase catalyst of the Stauffer type represented by point 3 $\sim 5 \times 10^{-6}$ for the onset of gas phase, we will have r in the macroparticle for diameter catalyst for the observed productivity, F $D_i = 10^{-5}$, $D_i \Phi_g = 10^{-6}$ $10^{-6} \leq D_i \leq 10^{-5}$ cm²/ in the macroparticle; h will be significant mass the particle size exceed:

Having shown that in the macroparticle un-analyze for macroparticle an isothermal particle. (37) has the solution

where z and α_i are diffusion factor, η_i , defined by eq.

From the definition of (41) and (42) graphically catalyst particles, one smaller catalyst particle size, growth factor Φ_g .

It is interesting to note in propylene slurry (e.g. size of 60 μ m), reasonable to cause macroparticle ductivity catalyst in gas not expect to see macro 10, where a catalyst polymerization with a high is true for high activity

temperature gradients in the macroparticle. However, note that a 60 μm diameter catalyst particle with the same observed productivity (point 2) will be expected to have negligible internal heat and mass transfer resistance for $D_l\Phi_g > 10^{-3}$. Thus if we assume $D_l = 10^{-4}$, then one would expect significant internal temperature and concentration gradients until the polymer had grown by a factor of 10 ($\Phi_g = 10$).

If we consider gas phase propylene polymerizations with a low activity catalyst of the Stauffer AA type with a catalyst diameter of 60 μm , this is represented by point 3 in Figure 9 corresponding to $D_l\Phi_g$, D_l values of $\sim 5 \times 10^{-5}$ for the onset of diffusion resistance. Thus since $D_l > 10^{-4}$ for gas phase, we will have negligible temperature and concentration gradients in the macroparticle for this catalyst in gas phase. If we use a 60 μm diameter catalyst for the slurry polymerization of propylene with the same observed productivity, R_{ob} , this corresponds to point 4 in Figure 9 where $D_l = 10^{-5}$, $D_l\Phi_g = 10^{-5}$ for the onset of diffusion resistance. For slurry $10^{-6} \leq D_l \leq 10^{-5} \text{ cm}^2/\text{s}$. Thus there will not be any temperature gradients in the macroparticle; however, with an actual value of $D_l \sim 10^{-6}$, there will be significant mass transfer resistance due to diffusion—at least until the particle size exceeds $\Phi_g > 10$.

Having shown that intraparticle temperature gradients will be negligible in the macroparticle under most normal operating conditions, we may now analyze for macroparticle mass transfer limitations in more detail assuming an isothermal particle. For this case, the macroparticle material balance (37) has the solution

$$c = \sinh(\alpha_l z) / z \sinh(\alpha_l)$$

where z and α_l are defined by Eq. (38). Thus, the macroparticle effectiveness factor, η_l , defined by eq. (39), has the solution⁴¹

$$\eta_l = \frac{3}{\alpha_l} \left[\frac{1}{\tanh(\alpha_l)} - \frac{1}{\alpha_l} \right] \quad (42)$$

From the definition of α_l , R_{ob} in eqs. (40) and (41) one may represent eqs. (41) and (42) graphically as shown in Figures 10–12. Note that, for larger catalyst particles, one expects more serious diffusion limitations than for smaller catalyst particles at the same growth factor. However, for a fixed catalyst particle size, diffusion limitations are reduced with increasing growth factor Φ_g .

It is interesting to note from Figure 11 that for a low activity catalyst in propylene slurry (e.g., Stauffer AA type catalyst with average catalyst size of 60 μm), reasonable values of D_l (e.g., 10^{-6} – $10^{-5} \text{ cm}^2/\text{s}$) are sufficient to cause macroparticle diffusion limitations. However, for the same productivity catalyst in gas phase (where $D_l \approx 10^{-4}$ – $10^{-3} \text{ cm}^2/\text{s}$), one would not expect to see macroparticle diffusion limitations. As indicated in Figure 10, where a catalyst particle size of $d_c = 20 \mu\text{m}$ is used for ethylene polymerization with a high activity catalyst, one sees that the same conclusion is true for high activity catalysts; i.e., the possibility of significant intra-

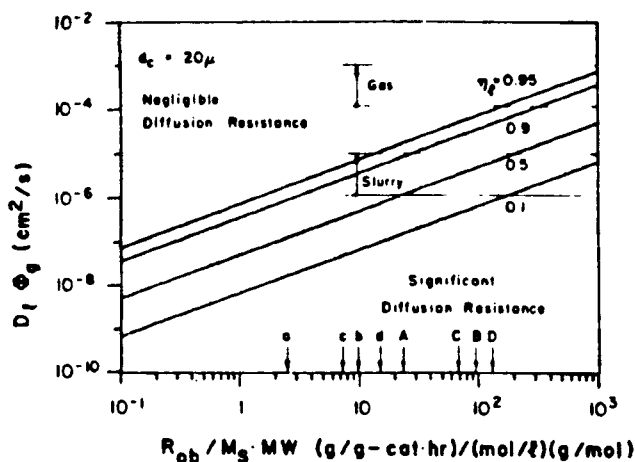


Fig. 10. Regimes for isothermal macroparticle diffusion resistance. $D_1\Phi_g$ vs. observed catalyst activity for catalyst with initial particle size $d_c = 20 \mu\text{m}$. Approximate values for typical catalyst if $M_s = M_p$: (a,A) propylene slurry polymerization, low and high activity catalyst; (b,B) propylene gas phase polymerization, low and high activity catalyst; (c,C) ethylene slurry polymerization, low and high activity catalyst; (d,D) ethylene gas phase polymerization, low and high activity catalyst (low activity, $R_{ob} = 400 \text{ g/g cat h}$, high activity, $R_{ob} = 4000 \text{ g/g cat h}$ under representative industrial conditions).

particle concentration gradients for slurry polymerization, but not for gas phase polymerization. However, as indicated in Figure 12, for gas phase polymerization with large high activity catalysts, internal concentration gradients can be significant. Furthermore, if catalyst activity continues to improve and catalyst particle sizes increase dramatically, then internal gradients will become even more significant in gas phase processes.

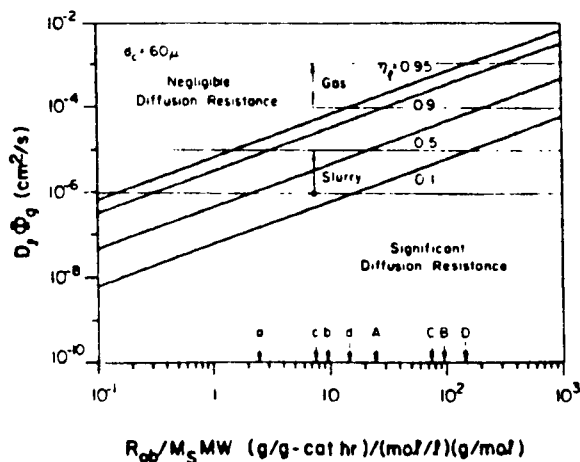


Fig. 11. Regimes for isothermal macroparticle diffusion resistance. $D_1\Phi_g$ vs. observed catalyst activity for catalyst with initial particle size $d_c = 60 \mu\text{m}$. Approximate values for typical catalysts if $M_s = M_p$: (a,A) propylene slurry polymerization, low and high activity catalyst; (b,B) propylene gas phase polymerization, low and high activity catalyst; (c,C) ethylene slurry polymerization, low and high activity catalyst; (d,D) ethylene gas phase polymerization, low and high activity catalyst (low activity, $R_{ob} = 400 \text{ g/g cat h}$, high activity, $R_{ob} = 4000 \text{ g/g cat h}$ under representative industrial conditions).

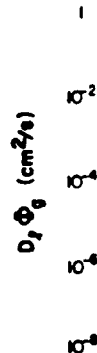


Fig. 12. Regimes for isothermal macroparticle diffusion resistance. $D_1\Phi_g$ vs. observed catalyst activity for catalyst with initial particle size $d_c = 20 \mu\text{m}$. Approximate values for typical catalyst if $M_s = M_p$: (a,A) propylene slurry polymerization, low and high activity catalyst; (b,B) propylene gas phase polymerization, low and high activity catalyst; (c,C) ethylene slurry polymerization, low and high activity catalyst; (d,D) ethylene gas phase polymerization, low and high activity catalyst (low activity, $R_{ob} = 400 \text{ g/g cat h}$, high activity, $R_{ob} = 4000 \text{ g/g cat h}$ under representative industrial conditions).

It is clear from Figure 12 that the diffusion resistance could manifest itself in gas phase polymerization, as has been reported for low activity catalyst. Note that for high activity catalyst and large particle size, the overall yield for high

In this paper quantitative estimates of M_s are given in graphical form to allow comparison of the effect of catalyst activity, temperature and particle size on the overall yield for high activity catalyst. Because of the large effect of catalyst activity, these criteria are more significant than particle size when there is a significant catalyst activity gradient. Similarly, macro- and micro-particle size estimates of M_s are more significant when there is a significant catalyst activity gradient. From the analysis of the effect of catalyst activity on the overall yield for high activity catalyst, it is clear that the temperature gradient across the macroparticles is more significant than the concentration gradient would be for large particle size. The overall yield for high activity catalyst would be for large particle size and high catalyst activity, the polymer particle size and catalyst activity concentration gradient.